

KINETIC FRACTIONATION OF THE ISOTOPE COMPOSITION OF ^{18}O , ^{13}C , AND OF CLUMPED ISOTOPE $^{18}\text{O}^{13}\text{C}$ IN CALCITE DEPOSITED TO SPELEOTHEMS. IMPLICATIONS TO THE RELIABILITY OF THE ^{18}O AND Δ_{47} - PALEOTHERMOMETERS

KINETIČNA FRAKCIJACIJA IZOTOPOV ^{18}O , ^{13}C IN IZOTOPSKEGA SKUPKA $^{18}\text{O}^{13}\text{C}$ V SIGAH IN ZANESLJIVOST PALEOTERMOMETROV ^{18}O IN Δ_{47}

Wolfgang DREYBRODT^{1,2}

Abstract

UDC 552.545:54.027

Wolfgang Dreybrodt: Kinetic fractionation of the isotope composition of ^{18}O , ^{13}C , and of clumped isotope $^{18}\text{O}^{13}\text{C}$ in calcite deposited to speleothems. Implications to the reliability of the ^{18}O and Δ_{47} paleothermometers

Kinetic fractionation of ^{18}O and clumped isotopes $^{13}\text{C}^{18}\text{O}$ in calcite precipitated to speleothems in cave environments renders the paleo-climatic interpretation of these proxies difficult.

Therefore a better understanding of the processes generating the isotope imprint is needed. A heuristic approach is taken to interpret recent data of the fractionations $\varepsilon_{\text{CaCO}_3-\text{HCO}_3}^{13,18}$ in a cave analogue experiment of calcite precipitation (Hansen *et al.* 2019) that shows a dependence on experimental precipitation rates, F . An expression, $\varepsilon_{\text{CaCO}_3-\text{HCO}_3}^{\text{kin}} = \varepsilon - \lambda \cdot c_{\text{eq}}^{\text{ab}} \cdot \alpha_{\text{prec}}^{\text{ab}} / F$, is derived that is based on uni-directional irreversible precipitation and is valid for large F when the forward rate of precipitation dominates the backward rate of dissolution. In that derivation it is assumed that the kinetic constants of precipitation rates are different for the different isotopologues and that this is also true for their equilibrium concentrations c_{eq} with respect to calcite. The constant, ε , is expressed by the kinetic fractionation $\varepsilon = 1 - \alpha_{\text{prec}}^{\text{rare}} / \alpha_{\text{prec}}^{\text{ab}}$ where α denote the rate constants of precipitation for the rare and abundant isotopologues. The second constant, λ , is determined by the differing equilibrium concentrations of HCO_3^- isotopologues with respect to calcite and the p_{CO_2} in the surrounding atmosphere. Fitting this expression to the experimental data one obtains the parameters ε and λ for different temperatures. Regarding these results the temporal evolution of $^{18}\delta_{\text{CaCO}_3}(t)$ and $\Delta_{47}(t)$ is discussed for the experimental conditions and for cave environments.

Izveček

UDK 552.545:54.027

Wolfgang Dreybrodt: Kinetična frakcionacija izotopov ^{18}O , ^{13}C in izotopskega skupka $^{18}\text{O}^{13}\text{C}$ v sigah in zanesljivost paleotermometrov ^{18}O in Δ_{47}

Kinetična frakcionacija ^{18}O in skupka $^{13}\text{C}^{18}\text{O}$ v kalcitu, ki se kot siga odlaga v jamskih okoljih, dela težave pri interpretaciji paleoklime na osnovi teh proksijev. Zato potrebujemo boljše razumevanje procesov, od katerih je odvisen izotopski zapis v sigah. V tem delu s heurističnim pristopom interpretiramo nedavno pridobljene podatke frakcionacij $\varepsilon_{\text{CaCO}_3-\text{HCO}_3}^{13,18}$. Podatki, pridobljeni ob izločanju kalcita v pogojih, podobnih jamskim, kažejo, da na frakcionacijo bistveno vpliva hitrost izločanja kalcita (Hansen *et al.* 2019). V pogojih, ko je izločanje bistveno hitreje od raztapljanja, velja zveza $\varepsilon_{\text{CaCO}_3-\text{HCO}_3}^{\text{kin}} = \varepsilon - \lambda \cdot c_{\text{eq}}^{\text{ab}} \cdot \alpha_{\text{prec}}^{\text{ab}} / F$. Pri izpeljavi te enačbe upoštevamo, da so kinetične konstante izločanja in ravnotežna konstanta kalcita različne za različne izotopologe. Konstanto ε lahko izrazimo s kinetično frakcionacijo $\varepsilon = 1 - \alpha_{\text{prec}}^{\text{rare}} / \alpha_{\text{prec}}^{\text{ab}}$, kjer je α konstanta izločanja za redke oziroma večinske izotopologe. Drugo konstanto λ dobimo iz razlik ravnotežnih koncentracij izotopologov HCO_3^- glede na kalcit in na atmosferski p_{CO_2} . S prilagajanjem izraza eksperimentalnim podatkom dobimo ε in λ pri različnih temperaturah. To omogoča obravnavo časovne odvisnosti $^{18}\delta_{\text{CaCO}_3}(t)$ in $\Delta_{47}(t)$ pri eksperimentalnih pogojih in v jamskem okolju. Rezultati so pomembni za razumevanje uporabnosti paleotermometra $1000\ln\alpha_{\text{CaCO}_3-\text{H}_2\text{O}}^{18}$ in hkrati pokažejo na vzrok različnih kalibracij, kot jih zasledimo v literaturi. Rezultate lahko uporabimo tudi za izotopske skupke $^{13}\text{C}^{18}\text{O}$ in kalibracijo Δ_{47} za kalcitno sigo. Članek predstavi nov pogled na iskanje splošno veljavne kalibracije paleotermometrov ^{18}O in Δ_{47} .

¹ Faculty of Physics and Electrical Engineering, University of Bremen, Germany

² Karst Research Institute ZRC SAZU, Titov trg 2, 6230 Postojna, Slovenia
e-mail: dreybrodt@t-online.de

Received/Prejeto: 01.09.2019

DOI: <https://doi.org/10.3986/ac.v48i3.7710>

This has implications to the application of $1000 \ln \alpha^{18}_{CaCO_3-H_2O}$ as a paleo-thermometer. It shows the reason why so many differing calibrations have been reported. These results analogously can be applied also to clumped isotopes $^{13}C^{18}O$ and the calibration of the Δ_{47} -thermometer with regard to speleothem calcite. In summary, a better understanding of the problems arising in the search for generally valid calibrations of ^{18}O and Δ_{47} paleo-thermometers is presented.

Key words: Calcium carbonate, ^{13}C and ^{18}O isotopes, clumped isotopes, kinetic fractionation between HCO_3^- and calcite, Δ_{47} paleothermometer.

Ključne besede: kalcit, izotopa ^{13}C in ^{18}O , izotopski skupki, kinetična frakcionacija med HCO_3^- in kalcitom, paleotermometer Δ_{47} .

INTRODUCTION

The isotope compositions of ^{13}C and ^{18}O in calcite precipitated inorganically to speleothems nowadays are widely used as proxies of paleo-climate (Fairchild & Baker 2012). To this end the temperature dependence of the calcite-water fractionation factor ($1000 \ln^{18} \alpha_{calcite-water}$) from theoretical, laboratory and cave studies has been suggested as calibration to the growth temperature of speleothems. In the ideal case when precipitation of the calcite proceeds at very low growth rates in isotope equilibrium the ^{18}O isotope composition reflects the temperature of growth. The calibration of this line has been constructed from two measurements of isotope fractionation factors $^{18}\alpha_{calcite-water}$ of calcites from Devils Hole and Laghetto Basso (Corchia Cave, Italy) that grow extremely slow with growth rate of $10^{-11} \text{ mmol cm}^{-2} \text{ s}^{-1}$ in isotope equilibrium at 33.7°C (Coplen 2007) and 7.9°C (Daeron *et al.* 2019). However, most calcite deposited in caves to speleothems or farmed to glass plates at known temperature and also synthetic calcite obtained from the laboratory exhibit fractionation $1000 \ln^{18} \alpha_{calcite-water}$ that deviates from the Coplen-Daeron line thus rendering its use as paleo-thermometer questionable. The reason is kinetic fractionation that depends on the difference of rate constants and equilibrium concentrations in the precipitation rate laws of calcium and bicarbonate for the different isotopologues with respect to calcite (Dreybrodt 2008, 2016; Dreybrodt & Scholz 2011).

Little is perceived in the community about the processes that determine the evolution of the isotope composition when water deposits calcite to a stalagmite. One usually assumes that classical Rayleigh distillation (Mook 2000) is active during precipitation of calcite. Using this concept a fractionation factor is found. If it deviates from the known equilibrium value, as is mostly the case, kinetic fractionation is inferred.

Recently Hansen *et al.* (2019) reported the evolution of the isotope composition of DIC and calcite deposited from a thin film of water super saturated with respect to calcite in a cave analogue experiment. They obtained values that deviated unsystematically from the equilibrium values and inferred kinetic fractionation without further explanation. These results have recently been analyzed and interpreted by a kinetic model (Dreybrodt 2019).

In a second step they have explored the evolution of the fractionations $^{13}\epsilon_{CaCO_3-HCO_3}$ and $^{18}\epsilon_{CaCO_3-HCO_3}$. They suggested a dependence of this fractionation on the corresponding precipitation rates of calcite. Here we present a heuristic model that explains their observations and sheds light into the meaning of kinetic fractionation. Using these results the reasons for the problems in using the ^{18}O and also the Δ_{47} paleothermometers are discussed.

DERIVATION OF EQUILIBRIUM AND KINETIC FRACTIONATION FACTORS

EQUILIBRIUM FRACTIONATION:

The equilibrium fractionation factor $\alpha_{\text{CaCO}_3-\text{HCO}_3^-}$ for the reaction $\text{Ca}^{2+} + 2\text{HCO}_3^- \rightleftharpoons \text{Ca}^{2+} + \text{CO}_3^{2-} + \text{HCO}_3^- + \text{H}^+ \rightleftharpoons \text{CaCO}_3 + \text{H}_2\text{CO}_3$ is derived as follows: The mass action law for this reaction reads

$$\frac{[\text{Ca}^{2+}] \cdot [\text{CO}_3^{2-}]^i}{[\text{CaCO}_3]^i} = K_s^i \quad (1)$$

and that for the reaction $\text{HCO}_3^- \rightleftharpoons \text{H}^+ + \text{CO}_3^{2-}$

$$\frac{[\text{HCO}_3^-]^i}{[\text{CO}_3^{2-}]^i \cdot [\text{H}^+]} = K_2^i \Rightarrow [\text{CO}_3^{2-}]^i = \frac{[\text{HCO}_3^-]^i}{[\text{H}^+] \cdot K_2^i} \quad (2)$$

By inserting Equation 2 into Equation 1 one has

$$\frac{[\text{Ca}^{2+}] \cdot [\text{HCO}_3^-]^i}{[\text{CaCO}_3]^i \cdot [\text{H}^+]} = K_s^i \cdot K_2^i \quad (3)$$

[] denote concentrations. In the carbon bearing species, i, refers to the rare and abundant isotopologue and the K^i denote the corresponding mass action constants that are slightly different for the rare and the abundant isotopologue. Dividing the expressions (eq. 3) for the rare and abundant isotopes one gets the equilibrium fractionation factor $\alpha_{\text{CaCO}_3-\text{HCO}_3}$ as defined by Mook (2000)

$$\frac{\frac{[\text{Ca}^{2+}] \cdot [\text{HCO}_3^-]^{ab}}{[\text{CaCO}_3]^{ab} \cdot [\text{H}^+]}}{\frac{[\text{Ca}^{2+}] \cdot [\text{HCO}_3^-]^{rare}}{[\text{CaCO}_3]^{rare} \cdot [\text{H}^+]}} = \frac{K_s^{ab} \cdot K_2^{ab}}{K_s^{rare} \cdot K_2^{rare}} = \frac{[\text{HCO}_3^-]^{ab}}{[\text{CaCO}_3]^{ab}} \cdot \frac{[\text{CaCO}_3]^{rare}}{[\text{CaCO}_3]^{ab}} = \frac{[\text{HCO}_3^-]^{ab}}{[\text{HCO}_3^-]^{rare}} \cdot \frac{[\text{CaCO}_3]^{rare}}{[\text{CaCO}_3]^{ab}} = \alpha_{\text{CaCO}_3-\text{HCO}_3}^{eq} \quad (4)$$

The equilibrium fractionation factor is related to mass action constants and depends solely on temperature. It is valid only for reactions in equilibrium.

KINETIC FRACTIONATION:

The isotopologues, i, of calcite are deposited with rates

$$F^i = \alpha_{prec}^i \cdot (c^i - c_{eq}^i) \quad (5a)$$

where, c^i , stands for $[\text{HCO}_3^-]^i$ (Buhmann & Dreybrodt 1985). The rate constants α_{prec}^i and the ratios c_{eq}^i / c^i of equilibrium concentrations, c_{eq}^i and the corresponding concentrations, c^i are slightly different for the two isotopologues, i, (Dreybrodt 2008; Dreybrodt & Scholz 2011; Dreybrodt 2016). The amount of CaCO_3 deposited after time T is obtained by integration

$$\int_0^T F^i(t) \cdot dt = \alpha_{prec}^i \int_0^T (c^i(t) - c_{eq}^i) \cdot dt \quad (5b)$$

In the experiment of Hansen *et al.* calcite is deposited to a glass plate at constant concentration. The amount of calcite deposited to the glass after time T from a solution with constant concentration, c^i , and constant precipitation rate, F^i , is $F^i \cdot T = \alpha_{prec}^i \cdot (c^i - c_{eq}^i) \cdot T$. Consequently one gets the kinetic fractionation

$$\alpha_{CaCO_3-HCO_3}^{kin} = \frac{\frac{[CaCO_3]^{rare}}{[CaCO_3]^{ab}}}{\frac{[HCO_3^-]^{rare}}{[HCO_3^-]^{ab}}} = \frac{\frac{\alpha_{prec}^{rare} \cdot (c^{rare} - c_{eq}^{rare}) \cdot T}{\alpha_{prec}^{ab} \cdot (c^{ab} - c_{eq}^{ab}) \cdot T}}{\frac{c^{rare}}{c^{ab}}} = \frac{\alpha_{prec}^{rare} \cdot (c^{rare} - c_{eq}^{rare})}{\alpha_{prec}^{ab} \cdot (c^{ab} - c_{eq}^{ab})} \cdot \frac{c^{ab}}{c^{rare}} = \alpha \cdot \frac{\left(\frac{c^{ab}}{c^{rare}} \cdot c^{rare} - \frac{c^{ab}}{c^{rare}} \cdot c_{eq}^{rare} \right)}{(c^{ab} - c_{eq}^{ab})} \quad (6)$$

Since $\frac{c_{eq}^{ab}}{c^{ab}} \approx \frac{c_{eq}^{rare}}{c^{rare}} = \gamma \cdot \frac{c_{eq}^{ab}}{c^{ab}}$ where γ is close to 1 and expresses the slight difference in the equilibrium concentrations, c_{eq}^i , Dreybrodt (2016) we finally get $\alpha_{CaCO_3-HCO_3}^{kin}$ as a function of the concentration, c , of HCO_3^- in the calcite precipitating solution.

$$\frac{\frac{[CaCO_3]^{rare}}{[CaCO_3]^{ab}}}{\frac{[HCO_3^-]^{rare}}{[HCO_3^-]^{ab}}} = \alpha_{CaCO_3-HCO_3}^{kin} = \frac{\alpha_{prec}^{rare} \cdot (c^{ab} - \gamma c_{eq}^{ab})}{\alpha_{prec}^{ab} \cdot (c^{ab} - c_{eq}^{ab})} = \alpha \frac{c^{ab} - \gamma c_{eq}^{ab}}{c^{ab} - c_{eq}^{ab}} \quad (7)$$

Using $\gamma = \lambda + 1$ where $\lambda \ll 1$ one can express $\alpha_{HCO_3-CaCO_3}^{kin}$ as function of $(c - c_{eq})$ or of the precipitation rate F by

$$\alpha_{CaCO_3-HCO_3}^{kin} = \frac{\alpha_{prec}^{rare}}{\alpha_{prec}^{ab}} \cdot \left(1 - \lambda \frac{c_{eq}}{c - c_{eq}}\right) = \frac{\alpha_{prec}^{rare}}{\alpha_{prec}^{ab}} \cdot \left(1 - \lambda \frac{c_{eq} \cdot \alpha_{prec}^{ab}}{F}\right) = \alpha \cdot \left(1 - \lambda \frac{c_{eq} \cdot \alpha_{prec}^{ab}}{F}\right) \quad (8)$$

Note that the dependence on F is artificial to facilitate comparison to experimental data. The relation $\alpha_{CaCO_3-HCO_3}^{kin} = \alpha \cdot (1 - \lambda \cdot c_{eq} / (c - c_{eq}))$ expresses the fact that during kinetic fractionation, in contrast to equilibrium fractionation, $\alpha_{CaCO_3-HCO_3}^{kin}$ depends on the pathway of the reaction that is specified by the actual concentration, c , and the end concentration c_{eq} .

With $\varepsilon = \alpha - 1$ and, $\varepsilon_{CaCO_3-HCO_3}^{kin} = \alpha_{CaCO_3-HCO_3}^{kin} - 1$, the fractionation can be written as

$$\varepsilon_{CaCO_3-HCO_3}^{kin} = \varepsilon - \lambda \frac{c_{eq} \cdot \alpha_{prec}^{ab}}{F} = \delta_{CaCO_3} - \delta_{HCO_3} \quad (9)$$

δ , ε , and λ are in ‰. Note that for high values of F , i.e., high supersaturation, $(c - c_{eq})$, the contribution of λ , resulting from differing, c_{eq}^i , becomes small whereas close to equilibrium it becomes dominant.

The rate law, $F^i = \alpha_{prec}^i \cdot (c^i - c_{eq}^i)$, comprises the forward reaction of precipitation with reaction rate, R_p , and the backward reaction of dissolution with reaction rate, R_b . The fractionation of DIC is controlled by the $CaCO_3$ dissolution/precipitation ratio R_b/R_f (DePaolo 2011). Fractionation varies between an equilibrium limit at $R_b/R_f = 1$ and a kinetic limit at $R_b/R_f = 0$. My derivation of kinetic fractionation is valid for $R_b/R_f < 0.1$ (DePaolo 2011).

In all the processes discussed so far it is only the mass difference between the light and heavy isotopologues that causes changes in the isotope composition of the HCO_3^- pool. Therefore clumped isotopes must obey the same rules with the consequence that all arguments given above apply also to clumped isotopes for all reactions between pools of differing carbonate species: CO_2 in the atmosphere, aqueous CO_2 , HCO_3^- , CO_3^{2-} , and calcite. Therefore all arguments given above apply also to the application of the temperature dependence of Δ_{47} as paleothermometer, as will be shown later in this work.

EVALUATION OF EXPERIMENTAL DATA

Recently Hansen *et al.* (2019) reported experimental values of the fractionation $\varepsilon_{\text{CaCO}_3-\text{HCO}_3}$ for both ^{13}C and ^{18}O . They measured the isotope composition of DIC in a water film supersaturated with respect to calcite that flows down an inclined marble plate under well constrained conditions. This water precipitates calcite. Consequently the HCO_3^- and the calcium concentrations drop with distance, x , from the input. This enables one to determine the precipitation rates, F , as a function of the distance x . In a second experiment an identical supersaturated solution flowing down a sand blasted glass plate as a water layer with the same depth and velocity as that on the limestone plate precipitates calcite onto this plate.

The authors measured the isotope composition of the DIC in the water flowing along the limestone plate at various distances, x . They also measured the isotope composition of the calcite deposited to the glass plate

at the same distances x . From the difference of $\delta_{\text{HCO}_3}(x)$ measured in the DIC along the marble plate and $\delta_{\text{CaCO}_3}(x)$ measured in the calcite deposited on the glass plate they calculate $\varepsilon_{\text{HCO}_3-\text{CaCO}_3}$. This method relies on the assumption that precipitation along the marble plate is identical to that of the glass plate. The authors provide arguments that this assumption should hold. They admit, however, that large errors are likely. This can be seen in Fig. 19 b, d of their work where $\varepsilon_{\text{CaCO}_3-\text{HCO}_3}$ remains constant along the plate in contrast to other results in this figure.

In future measurements the following protocol could avoid the problem. A degassed supersaturated solution with pH above 8 is used to create the water film running down a short glass plate with a flow distance of about 20 cm and flow velocity of about 0.1 cm/s. Input and output conductivities should not differ by more than 5% during the entire experiment. This warrants almost

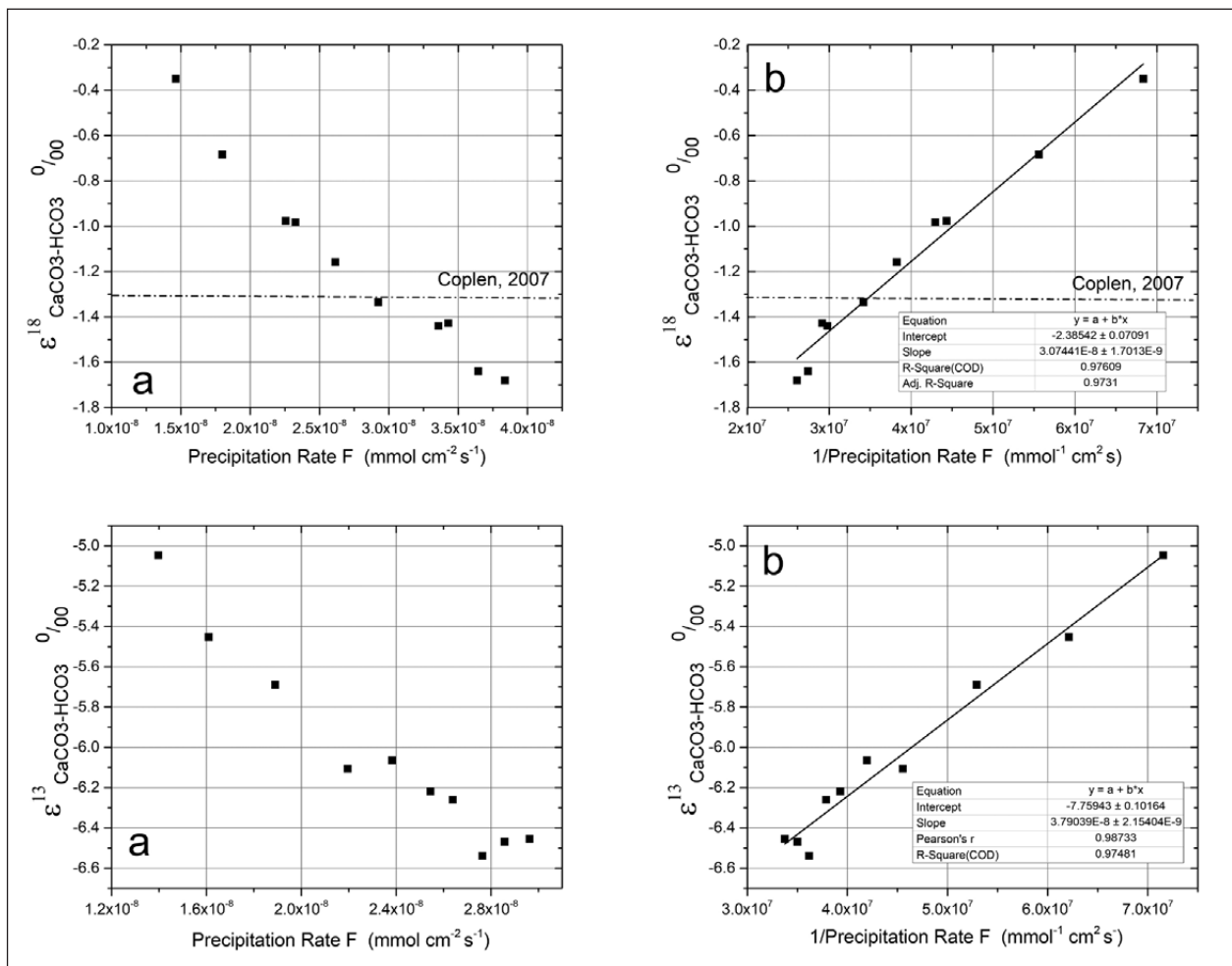


Fig. 1: Panels a) $\varepsilon_{\text{CaCO}_3-\text{HCO}_3}^{18}$ and $\varepsilon_{\text{CaCO}_3-\text{HCO}_3}^{13}$ as reported by Hansen *et al.* (2019). Panels b) Fits to Equation 9.

Tab. 1: Kinetic parameters ε and λ for ^{18}O and ^{13}C derived by use of Equation 9 from Fig. 19 and Fig. 16 in Hansen *et al.* (2019). c_{eq} is calculated using PHREEQC and the rate constant α_{prec} is taken from Fig. 2 in Baker *et al.* (1998).

Fig. in Hansen	P_{CO_2} (ppmV)	[Ca] (mmol/L)	T °C	ε ‰	λ ‰	c_{eq} (mmol/cm ³)	α_{prec} (cm/s)
^{18}O -19 a	1000	5	10	-3.2	-4.8	$0.93 \cdot 10^{-3}$	$1.1 \cdot 10^{-5}$
^{18}O -19 e	3000	5	20	-2.7	-3.8	$1.15 \cdot 10^{-3}$	$2.7 \cdot 10^{-5}$
^{18}O -19 h	1000	3	20	-2.4	-1.5	$0.78 \cdot 10^{-3}$	$2.7 \cdot 10^{-5}$
^{18}O -19 c	1000	5	30	-2.0	-2.5	$0.67 \cdot 10^{-3}$	$5.0 \cdot 10^{-5}$
^{18}O -19 f	3000	5	30	-3.4	-3.3	$0.97 \cdot 10^{-3}$	$5.0 \cdot 10^{-5}$
^{18}O -19 g	1000	5	30	-2.1	-6.3	$0.67 \cdot 10^{-3}$	$5.0 \cdot 10^{-5}$
^{13}C -16 a	1000	5	10	-7.5	-11.7	$0.93 \cdot 10^{-3}$	$1.1 \cdot 10^{-5}$
^{13}C -16 b	3000	5	10	-7.6	-3.8	$1.36 \cdot 10^{-3}$	$1.1 \cdot 10^{-5}$
^{13}C -16 c	1000	3	20	-7.7	-1.5	$1.15 \cdot 10^{-3}$	$2.7 \cdot 10^{-5}$
^{13}C -16 d	1000	2	30	-5.8	-1.3	$0.67 \cdot 10^{-3}$	$5.0 \cdot 10^{-5}$

even precipitation rates along the entire flow distance. At the start and at the end of the experiment the DIC in the solution at the input and in that flowing off at the end of the glass plate is precipitated as SrCO_3 to measure its isotope composition. When a sufficient amount of calcite has been precipitated the experiment is finished and the calcite is scratched off. Provided, that constant conditions have been assured $\varepsilon_{\text{CaCO}_3-\text{HCO}_3}$ can be calculated from $\delta_{\text{calcite}} - \delta_{\text{DIC}}$ in one single experiment. In addition the precipitation rate can be determined by the weight of the calcite deposited. The experiment must be performed with various Ca-concentrations to obtain differing precipitation rates.

The calcite precipitated from this experiment and the SrCO_3 obtained from DIC can also be used to measure Δ_{47} of calcite and DIC to obtain $\varepsilon_{\text{calcite HCO}_3}^{\text{clumped}}$. This may give important insights into kinetic fractionation of clumped isotopes.

In Fig. 16, Hansen *et al.* show $^{13}\varepsilon_{\text{CaCO}_3-\text{HCO}_3}$ as a function of precipitation rate F for various temperatures. In Fig. 19 correspondingly $^{18}\varepsilon_{\text{CaCO}_3-\text{HCO}_3}$ is reported.

I have used Equation 9 for fitting this data. In Fig. 1, panel a) data taken from Hansen *et al.* Fig. 19h are

shown. These were digitized by use of ORIGIN 2016. Fig. 1, panel b) depicts the same data plotted versus $1/F$. The full line is a linear fit to this data. The fitting parameters a (intercept) and b (slope) are listed in the box. From Equation 9 one reads $\varepsilon = a$ and $\lambda = -b$ ($c_{eq} \cdot \alpha_{prec}^{ab}$).

Similar fits were obtained for Fig. 19 a, d, e, f, g. The data in panel b) deviate from the general trend of other panels and have not been evaluated. In panels e) and f) some points deviated significantly from the general trend and were therefore omitted.

I have also used the data in Fig. 16 in Hansen *et al.* (2019) to evaluate $^{13}\varepsilon_{\text{CaCO}_3-\text{HCO}_3}$. An example is shown in the lower panels of Fig. 1. Satisfactory fits were obtained for all panels in Fig. 16. Tab. 1 lists the kinetic parameters ε and λ for all fits.

The kinetic parameters should monotonously depend on temperature solely. As one can see from Tab. 1 there is large scatter of the values of $^{18}\varepsilon$ and $^{18}\lambda$ for 30, 20, and 10°C. This indicates large errors in the experiments as admitted by Hansen *et al.* (2019). Nevertheless, the data indicates the validity of my approach. In the future more accurate experiments as suggested above are required.

DISCUSSION

TEMPORAL EVOLUTION OF Δ_{CaCO_3}

The isotope composition, $\delta_{\text{CaCO}_3}(t)$, of calcite precipitated to the glass plate after flow time, t , in the experiment is determined (Dreybrodt 2016) by

$$\delta_{\text{CaCO}_3}(t) = \delta_{\text{HCO}_3}(0) + \varepsilon_{\text{ray}}(t) + \varepsilon_{\text{HCO}_3-\text{CaCO}_3} \quad (10)$$

ε_{ray} is the increase of the isotope composition of HCO_3 by Rayleigh-distillation (Hansen *et al.* 2019). This is illustrated schematically in Fig. 2a. The bottom line stands for the isotope composition of HCO_3 , $\delta_{\text{HCO}_3}(0)$, at time zero.

In the experiments of Hansen *et al.*, DIC in the solution and the CO_2 in the surrounding atmosphere are in isotope equilibrium with the water. With increasing time, t , isotope composition, $\delta_{\text{HCO}_3}(t)$, increases by enrichment, $\varepsilon_{\text{ray}}(t)$, due to Rayleigh distillation along the flow path. The calcite deposited is enriched by, $\varepsilon_{\text{HCO}_3\text{-CaCO}_3}(t)$, that decreases with decreasing, $c\text{-}c_{\text{eq}}$. The dashed line depicts the value of $\delta_{\text{CaCO}_3}(\text{eq})$ when calcite is deposited in isotope equilibrium from a solution of chemical and isotope composition constant in time (Coplen 2007; Daeron *et al.* 2019). For details see Hansen *et al.* (2019).

In a cave environment the solution dripping to a stalagmite mostly has attained isotope equilibrium with the water (Dreybrodt & Scholz 2011) but not with the CO_2 in the cave atmosphere. Therefore, exchange with atmospheric CO_2 contributes

$$\delta^{\text{ex}}(t) = (\delta_{\text{eq}}^{\text{atm}} - \delta_0) \cdot t / \tau^{\text{ex}} \quad (11)$$

δ_0 is the initial value of DIC and $\delta_{\text{eq}}^{\text{atm}}$ that of DIC in isotope equilibrium with the cave CO_2 . Depending on the value of $\delta_{\text{eq}}^{\text{atm}}$, $\delta^{\text{ex}}(t)$ can be positive or negative. The exchange time τ^{ex} is at least one order of magnitude longer than the precipitation time of calcite (Dreybrodt *et al.* 2016; Dreybrodt & Romanov 2016; Hansen *et al.* 2017; Dreybrodt 2017). Therefore $\delta^{\text{ex}}(t)$ is small. If prior calcite precipitation (PCP) has been effective before the water impinges to the stalagmite Rayleigh distillation has already increased the isotope composition by $\varepsilon_{\text{ray}}^{\text{PCP}} > 0$. Regarding this one gets

$$\delta_{\text{CaCO}_3}(t) = \delta_{\text{HCO}_3}(0) + \varepsilon_{\text{PCP}} + \varepsilon_{\text{ex}}(t) + \varepsilon_{\text{ray}}(t) + \varepsilon_{\text{HCO}_3\text{-CaCO}_3}(t) \quad (12)$$

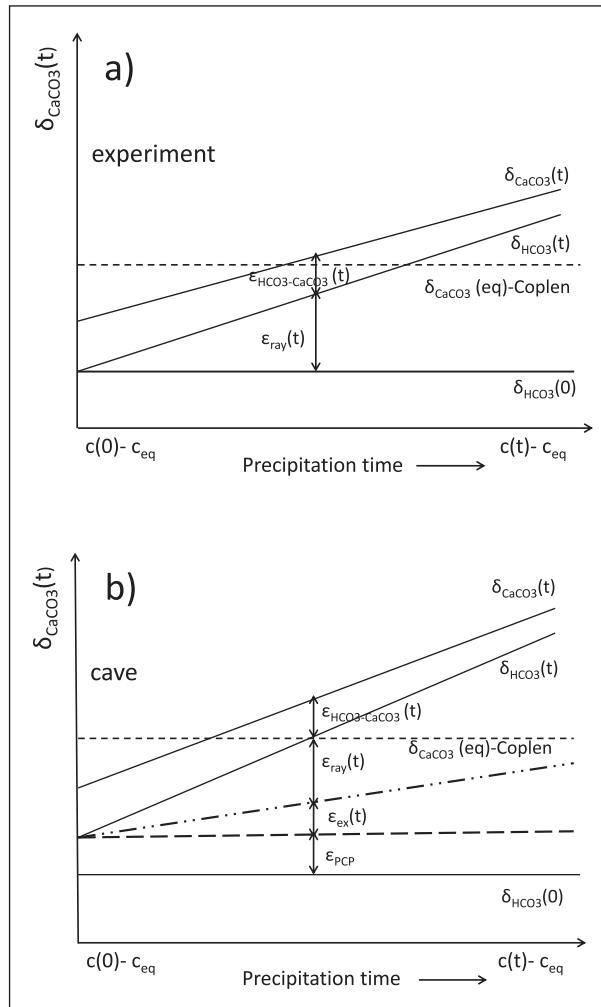


Fig. 2: Evolution of $^{18}\varepsilon_{\text{CaCO}_3/\text{HCO}_3}(t)$ in a calcite precipitating water film in the experiment (a) and (b) in natural conditions of a cave environment (see text).

as depicted in the lower panel of Fig. 2 illustrating these additional contributions. Note that δ_{CaCO_3} in the calcite deposited on a stalagmite is accumulated during the drip interval T_{drip} . Therefore δ_{CaCO_3} becomes correlated to T_{drip} and two stalagmites growing with differing drip intervals but under otherwise identical conditions from the same water source at the same time, close to each other may exhibit differing δ_{CaCO_3} when drip intervals, T_{drip} , were different. The question arises whether these stalagmites are suitable as paleo-climatic proxies. Only for drip intervals, $T_{\text{drip}} \ll \tau_{\text{prec}} \delta_{\text{CaCO}_3\text{-HCO}_3}(T_{\text{drip}}) - \delta_{\text{HCO}_3}(0)$ will be close to $\varepsilon_{\text{HCO}_3\text{-CaCO}_3}(0)$. The precipitation time of calcite is given by $\tau_{\text{prec}} = d / \alpha_{\text{prec}}^{\text{ab}}$ where, d , is the depth of the water layer on top of the stalagmite (Buhmann & Dreybrodt 1985). Stalagmites with diameters larger than 10 cm are suitable (Dreybrodt 2008). For high drip rates the water after entering the cave flows quickly to the stalagmite and there is little time for PCP. Therefore ε_{PCP} is small and can be neglected.

The evolution of δ_{CaCO_3} for both ^{13}C and ^{18}O is caused solely by the mass difference of the isotopologues. Therefore an analogue evolution is expected also for the clumped isotope $\text{Ca}^{13}\text{C}^{18}\text{O}^{16}\text{O}_2$ as the rare isotope and $\text{Ca}^{12}\text{C}^{16}\text{O}_3$ as the abundant one. From this one may define a δ_{clumped} in the traditional way that is related linearly to Δ_{47} , the common measure for clumped isotopes. As I will discuss later Rayleigh distillation and PCP cause negative changes in $\Delta_{47}(t)$ and accordingly also in $\delta_{\text{clumped}}(t)$. This is illustrated in Fig. 3. The evolution is similar to that in Fig. 2. But now δ_{clumped} decreases in time.

IMPLICATION TO THE CALIBRATION OF PALEOTHERMOMETERS

The $1000\ln\alpha^{18}_{CaCO_3-H_2O}$ paleothermometer

The dependence $\alpha^{18}_{CaCO_3-H_2O}$ on temperature for naturally and synthetically precipitated calcite has been suggested as a possible paleothermometer. $1000\ln\alpha^{18}_{CaCO_3-H_2O} = \epsilon_{H_2O-CaCO_3}$ is related to $\epsilon_{HCO_3-CaCO_3}$ by $\epsilon_{H_2O-CaCO_3} = \epsilon_{H_2O-HCO_3} + \epsilon_{HCO_3-CaCO_3}$. The fractionation $\epsilon_{H_2O-HCO_3}$ between water and HCO_3^- is a constant that depends on temperature solely (Beck *et al.* 2005). This means that $1000\ln\alpha^{18}_{CaCO_3-H_2O}$ must show the same variations as $\epsilon_{HCO_3-CaCO_3}$. Various attempts to calibrate $1000\ln\alpha^{18}_{CaCO_3-H_2O}$ as a paleothermometer for calcite precipitated naturally or synthetically have been reported.

Fig. 4 gives an overview. The upper panel illustrates various calibration lines taken from the literature.

The red dashed line is the equilibrium Daeron-Coplen calibration (Daeron *et al.* 2019). It represents fractionation in isotope equilibrium. This Daeron-Coplen line has been constructed from two isotope fractionation factors $\alpha_{calcite-water}$ of calcites from Devils Hole and Laghetto Basso (Corchia Cave, Italy) that grow extremely slow with growth rate of $10^{-11} \text{ mmol cm}^{-2} \text{ s}^{-1}$ in isotope equilibrium at 33.7°C (Coplen 2007) and 7.9°C respectively (Daeron *et al.* 2019).

The calibrations of Hansen *et al.* (2019) (black, dashed), Tremaine *et al.* (2011) (green solid), and Affek and Zaarur (2014) (magenta solid), all constructed from a variety of natural and synthetic calcites, are close to each other. The orange line is taken from the work of Johnston *et al.* (2013, Fig. 6). The lower panel illustrates the distribution of data points used for the construction of the orange Johnston line. Here a histogram of the differ-

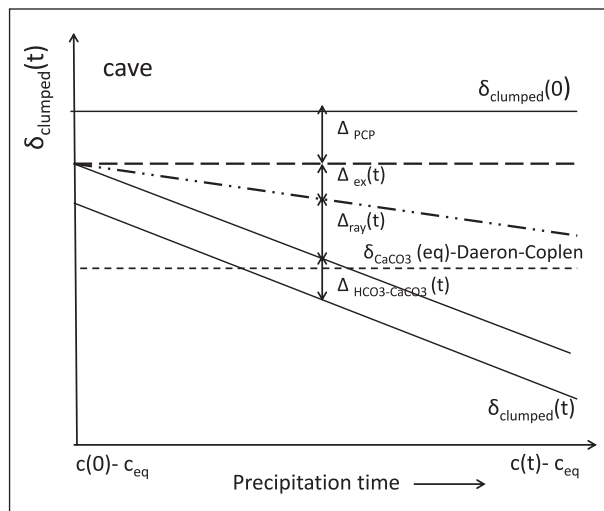


Fig. 3: Evolution of $\Delta_{17}(t)$ in a calcite precipitating water film in the natural conditions of a cave environment (see text).

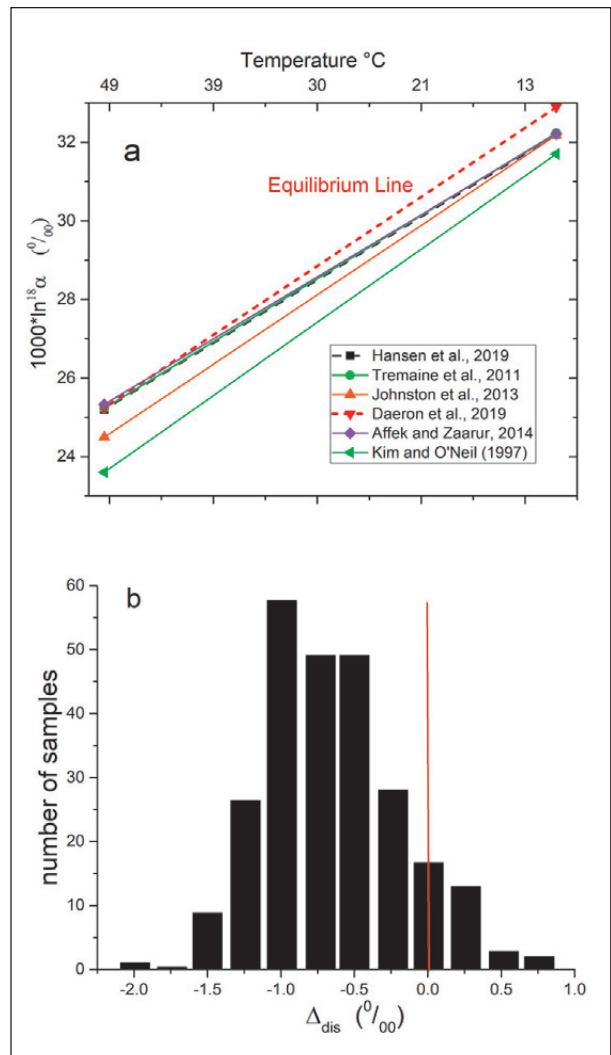


Fig. 4: a) $1000 \cdot \ln \alpha^{18}_{H_2O-CaCO_3}$ versus $1/T$ modified from Johnston *et al.* (2013). b) The distribution of data points used for the construction of the orange (Johnston) line in the upper panel. See text.

ence between the equilibrium line and the actual data points is constructed from the plot in Fig. 6 in Johnston *et al.* (2013).

It is important to note that most of the data points and calibration lines are below the Daeron-Coplen equilibrium calibration. This is also the case for the data of Feng *et al.* (2014) and also valid for experiments with synthetic calcite with growth rates of several $10^{-9} \text{ mmol cm}^{-2} \text{ s}^{-1}$ (Levitt *et al.* 2018) as can be seen from Fig. 6 in Johnston *et al.* (2013). It is evident that most of cave calcite is precipitated out of equilibrium with kinetic fractionation $\epsilon^{kin}_{HCO_3-CaCO_3}$ smaller than $\epsilon^{eq}_{HCO_3-CaCO_3}$.

Yan *et al.* (2012) investigated $\delta^{18}\text{O}$ in calcite precipitated in pools and in streams with fast flow in a low-

temperature travertine-depositing system at Baishuitai, Yunnan, SW China (Yan *et al.* 2012).

They found that the $\delta^{18}\text{O}$ values of travertine precipitated in the canal system increased downstream, recording the $\delta^{18}\text{O}$ values of dissolved carbonates (HCO_3^-) in the stream water that augmented by Rayleigh-distillation along the canal. However, in the pool systems with slow flow and almost stagnant water pools of large volume where carbonate concentration is constant in time, oxygen isotope equilibrium between dissolved carbonates and H_2O was achieved. The $\delta^{18}\text{O}$ values of travertine deposited there with rates lower by a factor of ten compared to the rates in the stream water were in agreement with those calculated from the equilibrium Daeron-Coplen calibration. This is what one expects from Fig. 2.

Generally, one anticipates that calcite precipitated from large volumes of water where the DIC concentration stays constant in time should be in isotope equilibrium and consequently $1000 \cdot \ln^{18}\alpha_{\text{H}_2\text{O}-\text{CaCO}_3}$ and Δ_{47} of calcite precipitated under such conditions should be close to the value of the corresponding Daeron-Coplen calibration. In such large water bodies with depth, a , of at least onecm isotope exchange with the surrounding atmosphere is slow because the exchange time τ_{ex} proportional to a/D where, D , the coefficient of molecular diffusion of CO_2 is $2 \cdot 10^{-5} \text{ cm}^2 \text{ s}^{-1}$ (Dreybrodt *et al.* 2016). For a depth, a , of 1 cm τ_{ex} is on the order of 1 year. Since the amount of calcite precipitated is so little that the concentration of DIC stays unaltered Rayleigh distillation is excluded. In Figs. 2 and 3 this means that precipitation happens at $c(0) = c_{\text{eq}}$ in isotope equilibrium of all species involved.

Recently Breitenbach *et al.* (2018, 2019) have reported a calibration of “*subaqueously-precipitated carbonates (SPC) which form in cave pools and drip sites, as well as natural hot springs. SPC include cave pearls, cave*

pool rim carbonates, hot spring pisoids, and carbonate geodes. Clumped isotope measurements confirmed isotopic equilibrium for both, $\delta^{18}\text{O}$ and Δ_{47} of the analysed SPCs, supporting the equilibrium equations of Coplen”. The calibration of Δ_{47} is presented in Breitenbach *et al.* (2018). It is shown in Fig. 5 and is very close to the Daeron-Coplen equilibrium calibration line.

In contrast to the SPC, calcite deposited to stalagmites from thin layers of water exhibits values of $1000 \cdot \ln^{18}\alpha_{\text{H}_2\text{O}-\text{CaCO}_3}$ and Δ_{47} that are out of equilibrium (Tremaine *et al.* 2011). Keeping in mind that now calcite precipitates from a solution with a small volume such that the Ca- and DIC concentrations change on time scales of hundred seconds this can be explained as follows: For water that has not yet precipitated calcite when it drips to the stalagmite with drip intervals small compared to the precipitation time ($\tau_{\text{drip}} \ll \tau_{\text{prec}}$) the enrichment of the heavy isotope can be neglected because $\varepsilon_{\text{ray}}(\tau_{\text{drip}})$ and $\varepsilon_{\text{ex}}(\tau_{\text{drip}})$ are close to zero (Dreybrodt 2016; Dreybrodt & Romanov 2016). If, however drip intervals are sufficiently long such that the HCO_3^- concentration is reduced significantly the contribution of Rayleigh distillation, ε_{ray} , and that of exchange, ε_{ex} , cannot be neglected and the calibration points for a given temperature will depend on the drip interval. In other words, $1000 \ln \alpha_{\text{CaCO}_3-\text{H}_2\text{O}}^{18}$ depends on drip interval and therefore calcites precipitated at the same temperature may exhibit different values of $1000 \ln \alpha_{\text{CaCO}_3-\text{H}_2\text{O}}^{18}$.

If prior calcite precipitation (PCP) has been effective before the water impinges to the stalagmite Rayleigh distillation has already increased the isotope composition by $\varepsilon_{\text{ray}}^{\text{PCP}} > 0$. Most of the points are below the Coplen-Daeron line. In some favorable cases the total enrichment $\varepsilon_{\text{tot}} = \varepsilon_{\text{ray}} + \varepsilon_{\text{ex}} + \varepsilon_{\text{ray}}^{\text{PCP}} > 0$ may be sufficiently large to put the point above the Coplen-Daeron line.

Note that in the experiments of Hansen *et al.* (2019), Fig. 19 therein and Fig. 1 in this work due to the action of Rayleigh distillation calcite deposited close to the output of the glass plate exhibits δ values close to the Daeron-Coplen line and above it. This implies that calcite that carries an isotope imprint close to that of the equilibrium line has not necessarily been precipitated in isotope equilibrium.

Experiments have been reported to constrain the value of $\alpha_{\text{CaCO}_3-\text{H}_2\text{O}}^{18,\text{eq}}$ with respect to precipitation rates. Dietzel *et al.* (2009) observed $\alpha_{\text{CaCO}_3-\text{H}_2\text{O}}^{18}$ values at pH of 8.3 and 10°C, 20°C, and 30°C with precipitation rates between $5.8 \cdot 10^{-9} \text{ mmol cm}^{-2} \text{ s}^{-1}$ and $5.8 \cdot 10^{-7} \text{ mmol cm}^{-2} \text{ s}^{-1}$. The values decrease with increasing precipitation rate. Recently Levitt *et al.* (2018) reported $\alpha_{\text{CaCO}_3-\text{H}_2\text{O}}^{18}$ of synthetic calcite precipitated close to equilibrium with rates between 10^{-9} and $10^{-8} \text{ mmol cm}^{-2} \text{ s}^{-1}$.

Watkins *et al.* (2014) proposed a model that rep-

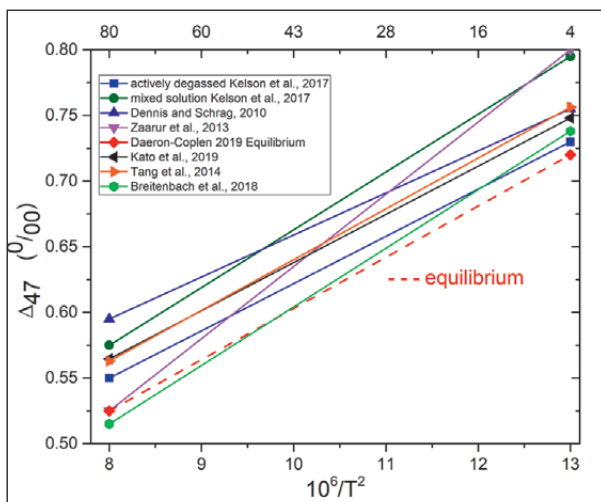


Fig. 5: Δ_{47} versus $10^6/T^2$ modified from Kelson *et al.* (2017). See text.

resents the effects of ion-by-ion growth of calcite and describes the dependence of $\alpha^{18}_{CaCO_3-H_2O}$ on growth rates between the equilibrium limit at extremely slow growth at several 10^{-11} mmol cm⁻² s⁻¹ and the kinetic limit for growth rates higher than $2 \cdot 10^{-8}$ mmol cm⁻² s⁻¹. This model shows good agreement with their experimental data.

It is difficult to interpret these findings with my model because c_{eq} and α_{prec} are not well constrained in these experiments and the errors in the rate dependence on precipitation rates are high.

The experiments of Hansen *et al.* (2019) performed with rates of several 10^{-8} mmol cm⁻² s⁻¹ must be assigned to the kinetic limit and are well constrained with respect to the chemical, c_{eq} , and kinetic, α_{prec} , conditions of the precipitation. Therefore they can be described by Equation 9.

The clumped isotope Δ_{47} thermometer

As stated above the Δ_{47} -thermometer should show a similar behavior as the $1000\ln\alpha^{18}_{CaCO_3-H_2O}$ paleothermometer. Here also deviations from the Coplen-Daeron equilibrium line are observed. Fig. 5, modified from Fig. 5 in Kelson *et al.* (2017) illustrates these findings. I have also added the calibration by Tang *et al.* (2014) from inorganic calcites grown under well-controlled experimental conditions and that of Kato *et al.* (2019) derived from synthetic calcite. The red dashed line depicts the Δ_{47} -Daeron-Coplen equilibrium calibration line taken from Daeron *et al.* (2019). The green line depicts the calibration of Breitenbach *et al.* (2018) derived from subaqueous precipitated calcites as discussed above. As one expects it is very close to the equilibrium line although with slightly different slope.

All the other calibration lines exhibit values higher than those of the Δ_{47} Daeron-Coplen equilibrium line because the positive Rayleigh distillation effect for ¹⁸O is accompanied by a negative change of Δ_{47} . The Δ_{47} offset per 1 ‰ of $\delta^{18}O$ is about -0.02 ‰ (Affek & Zaarur 2014; Guo, 2019; Guo & Zhou 2019). Theoretical calculations of Guo (2008) indicate a reduction of 0.0175–0.029‰ in Δ_{47} for each 1‰ increase in $\delta^{18}O$. Kluge *et al.* (2013) observed an offset of -0.047 in speleothems from Bunker Cave (Germany). The consequences are illustrated in Fig. 3. In analogy to Fig. 2, PCP and Rayleigh distillation cause shifts from $\delta_{clumped}$ that now, however are negative. This is the reason why in Fig. 5 the calibration lines exhibit values higher than that of the equilibrium line.

One might argue that the departure from equilibrium may be restored by quick equilibration. This argument, however, does not hold. In a recent paper Weise and Kluge (2020) report on the kinetics of the temporal evolution $\delta^{18}O$ and Δ_{47} in the DIC pool of sodium bicarbonate solutions at pH 8 and temperatures of 40°C, 55°C, 70°C, and 90°C that are out of isotope equilibrium. These achieve isotope equilibrium by exponential approach with time constant, $\tau_{eq} = 1 / \exp(-10^4/T + 29)$, where T is in °K and τ_{eq} in minutes. The long relaxation times of 55 min at 30°C, 160 min at 20°C, and 570 min at 10°C are much larger than the precipitation time τ_{prec} of about 14 min at 30°C, 25 min at 20 °C, and 70 min at 10°C (Baker *et al.* 1998) and equilibration is of little influence.

All these arguments give evidence why many of the various calibration lines of $1000\ln\alpha^{18}_{CaCO_3-H_2O}$ and Δ_{47} differ from each other and cannot be used reliably as a paleothermometer for calcite precipitated to speleothems.

CONCLUSION

A heuristic approach is presented to interpret recent data of kinetic fractionation $^{13}\epsilon^{kin}_{CaCO_3-HCO_3}$ and $^{18}\epsilon^{kin}_{CaCO_3-HCO_3}$ in cave analogue experiments by Hansen *et al.* (2019). Two parameters $\epsilon = 1 - \alpha$ and λ are needed to explain kinetic fractionation that depends on the growth rates of the calcite precipitated. α is the ratio of the rate constants of precipitation for the rare and abundant isotope and λ expresses the fact that the equilibrium concentration, c_{eq} , of HCO_3^- with respect to calcite differs for the rare and abundant isotope. This approach is different from prior interpretations that infer kinetic fractionation whenever the fractionation ϵ is different from that expected for equilibrium fractionation.

In view of these results the origin of the isotope compositions $\delta^{13,18}_{CaCO_3}$ for the experiments of Hansen *et al.* (2019) and for the environment in a cave is discussed and an explanation is given why most of calcite precipitated to stalagmites has values of $1000\ln\alpha^{kin}$ less than that what is expected for equilibrium by the calibration of Coplen (2007) and Daeron *et al.* (2019).

These results show why it is difficult to find a general valid calibration line for most naturally precipitated calcites. Analogue arguments apply to the understanding of problems with the Δ_{47} -thermometer. An improved set up for future cave analogue experiments to measure $^{13,18}\epsilon^{kin}_{CaCO_3-HCO_3}$ and Δ_{47} more reliably is suggested.

ACKNOWLEDGEMENT

This work was performed in connection to grant DR 79/14-1 (DFG). I acknowledge support by the Deutsche Forschungsgemeinschaft (DFG). Discussions with Tobias Kluge are highly appreciated.

REFERENCES

- Affek, H.P. & S. Zaarur 2014: Kinetic isotope effect in CO_2 degassing: Insight from clumped and oxygen isotopes in laboratory precipitation experiments.- *Geochimica et Cosmochimica Acta*, 143, 319–330. DOI: 10.1016/j.gca.2014.08.005
- Baker, A., Genty, D., Dreybrodt, W., Barnes, W. L., Mockler, N. J. & J. Grapes, 1998: Testing theoretically predicted stalagmite growth rate with recent annually laminated stalagmites: implications for past stalagmite deposition.- *Geochimica et Cosmochimica Acta* 62, 393–404. DOI: 10.1016/S0016-7037(97)00343-8
- Beck, W.C., Grossman, E.L., & J.W., Morse 2005. Experimental studies of oxygen isotope fractionation in the carbonic acid system at 15°, 25°, and 40 °C. *Geochim. Cosmochim. Acta* 69, 3493–3503.
- Breitenbach, S. F.M., Hartland, A., Brall, N. S., Sharp, W. D., Sanchez, F. G., Rolfe, J., Bernasconi, S. M. & D.A. Hodell, 2019: Closing in on the oxygen isotopic fractionation factor between calcite and water using natural carbonates.- *Geophysical Research Abstracts*, 21, EGU2019-6196.
- Breitenbach, S. M. F., Mleneck-Vautravers, M. J., Grauel, A.-L., Bernasconi, S. M., Müller, I. A., Rolfe, J., Gazquez, F., Greaves, M. & D.A. Hodell, 2018: Coupled Mg/Ca and clumped isotope analyses of foraminifera provide consistent water temperatures. *Geochimica et Cosmochimica Acta*, 236, 283–296. DOI:10.1016/j.gca.2018.03.010
- Buhmann, D. & W. Dreybrodt 1985: The kinetics of calcite dissolution and precipitation in geologically relevant situations of karst areas: I. Open system.- *Chemical Geology*, 48, 189–211. DOI: 10.1016/0009-2541(85)90024-5.
- Coplen, T. B., 2007: Calibration of the calcite-water oxygen-isotope geothermometer at Devils Hole, Nevada, a natural laboratory.- *Geochim. Cosmochim. Acta*, 71, 3948–3957. DOI: 10.1016/j.gca.2007.05.028
- Daeron, M., Drysdale, R.N., Peral, M., Huyghe, D., Blamartm D., Coplen, T.B., Lartaud, F. & G. Zanchetta, 2019: Most Earth-surface calcites precipitate out of isotopic equilibrium.- *Nature Communications*, 10, 429. DOI: 10.1038/s41467-019-08336-5
- Dennis, K. J. & D.P. Schrag, 2010: Clumped isotope thermometry of carbonatites as an indicator of diagenetic alteration.- *Geochimica et Cosmochimica Acta*, 74, 4110–4122. DOI: 10.1016/j.gca.2010.04.005
- DePaolo, D. J., 2011: Surface kinetic model for isotopic and trace element fractionation during precipitation of calcite from aqueous solutions.- *Geochimica et Cosmochimica Acta* 75, 1039–1056. DOI: 10.1016/j.gca.2010.11.020
- Dietzel, M., Tang, J., Leis, A. & S.J. Kohler, 2009: Oxygen isotopic fractionation during inorganic calcite precipitation – Effects of temperature, precipitation rate and pH.- *Chem. Geol.*, 268, 107–115. DOI: 10.1016/j.chemgeo.2009.07.015
- Dreybrodt, W., 2017: Isotope exchange between DIC in a calcite depositing water layer and the CO_2 in the surrounding atmosphere : Resolving a recent controversy.- *Acta carsologica*, 46/2–3, 339–345. DOI: 10.3986/ac.v46i2-3.6597
- Dreybrodt, W., 2019: Physics and chemistry of CO_2 outgassing from a solution precipitating calcite to a speleothem: Implication to ^{13}C , ^{18}O , and clumped $^{13}\text{C}^{18}\text{O}$ isotope composition in DIC and calcite.- *Acta Carsologica*, 48/1, 59-68. DOI: /10.3986/ac.v48i1.7208
- Dreybrodt, W. & D. Romanov, 2016: The evolution of ^{13}C and ^{18}O isotope composition of DIC in a calcite depositing film of water with isotope exchange between the DIC and a CO_2 containing atmosphere, and simultaneous evaporation of the water. Implication to climate proxies from stalagmites: A theoretical model.- *Geochimica et Cosmochimica Acta*, 195, 323-338. DOI: 10.1016/j.gca.2016.07.034.
- Dreybrodt, W., Hansen M. & D. Scholz, 2016: Processes affecting the stable isotope composition of calcite during precipitation on the surface of stalagmites: Laboratory experiments investigating the isotope exchange between DIC in the solution layer on top of a speleothem and the CO_2 of the cave atmosphere. - *Geochimica et Cosmochimica Acta*, 174, 247–262. DOI: 10.1016/j.gca.2015.11.012.
- Fairchild, I. J. & A. Baker, 2012: *Speleothem Science: From Process to Past Environments*.-Wiley-Blackwell. pp. 450.

- Feng, W., Casteel, R. C., Banner, J. L. & A. Heinze-Fry, 2014: Oxygen isotope variations in rainfall, drip-water and speleothem calcite from a well-ventilated cave in Texas, USA: Assessing a new speleothem temperature proxy.- *Geochimica et Cosmochimica Acta*, 127, 233–250. DOI: 10.1016/j.gca.2013.11.039
- Guo, W., 2008: Carbonate clumped isotope thermometry: application to carbonaceous chondrites & effects of kinetic isotope fractionation.- Ph. D. thesis, California Inst. Techn., pp. 261.
- Guo, W., 2019: Kinetic clumped isotope fractionation in the DIC-H₂O-CO₂ system: Patterns, controls, and implications.- *Geochimica et Cosmochimica Acta*, in press. DOI: 10.1016/j.gca.2019.07.055
- Guo, W. & C. Zhou, 2019: Patterns and Controls of Disequilibrium Isotope Effects in Speleothems: Insights from an Isotope-Enabled Diffusion-Reaction Model and Implications for Quantitative Thermometry.- *Geochimica et Cosmochimica Acta*, in press. DOI: 10.1016/j.gca.2019.07.028
- Hansen, M., Scholz, D., Froeschmann, M.-L., Schöne, B.R. & C. Spötl, 2017: Carbon isotope exchange between gaseous CO₂ and thin solution films: Artificial cave experiments and a complete diffusion-reaction model.- *Geochim. Cosmochim. Acta* 211, 28–47. DOI: 10.1016/j.gca.2017.05.005
- Hansen, M., Scholz D., Schöne B. R. & C. Spötl, 2019: Simulating speleothem growth in the laboratory: Determination of the stable isotope fractionation ($\delta^{13}\text{C}$ and $\delta^{18}\text{O}$) between H₂O, DIC and CaCO₃. -*Chemical Geology* 509, 20-44. DOI: 10.1016/j.chemgeo.2018.12.012
- Johnston, V. E., Borsato, A., Spötl, C., Frisia, S. & R. Miorandi, 2013: Stable isotopes in caves over 3: altitudinal gradients: fractionation behaviour and inferences for speleothem sensitivity to climate change.- *Climate of the Past*, 9, 99–118. DOI: 10.5194/cp-9-99-2013
- Kato, H., Amekawa, S., Kano, A., Mori, T., Kuwahara, Y. & J. Quade, 2019: Seasonal temperature changes obtained from carbonate clumped isotopes of annually laminated tufas from Japan: Discrepancy between natural and synthetic calcites.- *Geochimica et Cosmochimica Acta*, 244, 548–564. DOI: 10.1016/j.gca.2018.10.016.
- Kelson, J. R., Huntington, K. W., Schauer, A. J., Saenger, C. & A.R. Lechler, 2017: Toward a universal carbonate clumped isotope calibration: Diverse synthesis and preparatory methods suggests single temperature relationship.- *Geochimica et Cosmochimica Acta*, 197, 104–131. DOI: 10.1016/j.gca.2016.10.010
- Kim, S.-T. & J.R O'Neil, 1997: Equilibrium and nonequilibrium oxygen isotope effects in synthetic carbonates.- *Geochimica et Cosmochimica Acta*, 61, 3461–3475. DOI: 10.1016/S0016-7037(97)00169-5
- Kluge, T., Affek, H. P., Marx, T., Aeschbach-Hertig, W., Riechelmann, D. F. C., Scholz, D., Riechelmann, S., Immenhauser, A., Richter, D.K., Fohlmeister, J., Wackerbarth, A., Mangini, A. & C. Spötl, 2013: Reconstruction of drip-water $\delta^{18}\text{O}$ based on calcite oxygen and clumped isotopes of speleothems from Bunker Cave (Germany).- *Climate of the Past*, 9, 377–391. DOI: 10.5194/cp-9-377-2013
- Levitt, N. P., Eiler, J. M., Romanek, C. S., Beard, B. L., Xu, H. & C.M. Johnson, 2018: Near equilibrium ^{13}C - ^{18}O bonding during inorganic calcite precipitation under chemo-stat conditions.- *Geochemistry, Geophysics, Geosystems*, 19, 901–920. DOI: 10.1002/2017GC007089
- Mook, W.G., 2000: *Environmental Isotopes in the Hydrological Cycle. Vol 1: Principles and Applications Vol.1*.-International Atomic Energy Agency and United Nations Educational, Scientific and Cultural Organization.- [Online] Available from: http://www.hydrology.nl/images/docs/ihp/Mook_I.pdf [Accessed January 30th 2019].
- Tang, J., Dietzel, M., Alvaro Fernandez, A., Aradhna, K., Tripathi, A. & B. E. Rosenheim, 2014: Evaluation of kinetic effects on clumped isotope fractionation (Δ_{47}) during inorganic calcite precipitation.- *Geochimica et Cosmochimica Acta* 134, 120–136. DOI: 10.1016/j.gca.2014.03.005
- Tremaine, D. M., Froelich, P.N. & Y. Wang, 2011: Speleothem calcite farmed in situ: Modern calibration of $\delta^{18}\text{O}$ and $\delta^{13}\text{C}$ paleoclimate proxies in a continuously monitored natural cave system.- *Geochim. Cosmochim. Acta* 75, 4929–4950. DOI:10.1016/j.gca.2011.06.005
- Watkins, J. M., Hunt, J.D., Ryerson, F. J. & D.J. DePaolo, 2014: The influence of temperature, pH, and growth rate on the $\delta^{18}\text{O}$ composition of inorganically precipitated calcite.- *Earth and Planetary Science Letters*, 404, 332–343. DOI: 10.1016/j.epsl.2014.07.036
- Weise, A. & T. Kluge, 2020: Isotope exchange rates in dissolved inorganic carbon between 40°C and 90°C.- *Geochimica et Cosmochimica Acta*, 268, 56–72, DOI: 10.1016/j.gca.2019.09.032
- Yan, H., Sun, H. & Z. Liu, 2012: Equilibrium vs. kinetic fractionation of oxygen isotopes in two low-temperature travertine-depositing systems with differing hydrodynamic conditions at Baishuitai, Yunnan, SW China.- *Geochimica et Cosmochimica Acta* 95, 63–78. DOI: 10.1016/j.gca.2012.07.024
- Zaarur, S., Affek, H. P. & M.T. Brandon, 2013: A revised calibration of the clumped isotope thermometer.- *Earth and Planetary Science Letters*, 382, 47–57. DOI: 10.1016/j.epsl.2013.07.026